Parametric Model of Gyroscopes

Svitlana Sotnik[1], Mohammad Ayaz Ahmad[2], Nataliya V. Belova[3], Vyacheslav Lyashenko[3]

[1]Department of Computer-Integrated Technologies, Automation and Mechatronics, Kharkiv National University of RadioElectronics, Kharkiv, Ukraine

[2]Department of Physics, Faculty of Science, P.O. Box 741, University of Tabuk, 71491, Tabuk, Saudi Arabia

[3]Department of Informatics, Kharkiv National University of Radio Electronics, Kharkiv, Ukraine

Abstract: The classification of gyroscopes based on the parametric model is considered. It is shown that the proposed parametric model can be used as a basis for developing a mathematical model in the process of creating a module for the automated vibration gyroscopes design, mechanical or optical type. Investigations of the failure probability and the failure-free operation probability for a period of 50 hours to 150 hours and for a period of 200 hours to 400 hours were conducted. Parameters and graphical representation of computational models are given.

Keywords: Gyroscope, Construction, Parametric Model, Trouble-free Operation, Failure-free Operation Probability.

INTRODUCTION

There are a number of fairly accurate gyroscopic systems that satisfy a large number of consumers [1-3]. For example, the micromechanical gyroscopes use, in vehicle stabilization systems or video cameras [4-6]. Nevertheless, the ever-increasing demands on the accuracy and gyroscopic instruments performance characteristics become a prerequisite not only for subsequent improvements to classical gyroscopes, but also for searching for fundamentally new ideas that allow solving the creating sensitive sensors problem for indicating and measuring the angular movements of an object in space.

At the present time, a large number of various phenomena and physical principles are known that allow solving problems arising in the gyroscopes design [7]. But there are also a number of questions. These issues include: construction design, calibration and effective use of gyroscopes. However, up to now these issues have not been fully resolved.

Among the most popular gyroscopes are micromechanical gyroscopes (MMG) [7]. The demand for such gyros is supported by many markets – client, medical, industrial and military [8].

The micromechanical gyro-accelerometer is also manufactured industrially in the form of small integrated circuits. Due to the miniaturized dimensions and relatively cheap cost of manufacturing this device, the MMG field application is growing every year [2]. But at the same time, the task remains to improve information reliability and ensure trouble-free operation of gyroscopes. At the same time, scientific and technical directions are actively developing, which are associated with the small-size motion control devices creation, where MMGs play a decisive role.

MATERIALS AND METHODS
Review of the literature on the research topic

The basic principles of the micromechanical gyroscopes design are set forth in the Yilmaz E study [10]. In this paper, the latest theoretical methodologies for analysis and various types design are presented; most attention is paid to the vibration Coriolis gyroscopes. The principles of designing sensors and their kinematics, origin of the motion equations, analyzing the sensors dynamics in modulated and demodulated signals, calculating and optimizing the main operating characteristics, and signal processing and control are also analyzed. In [10], numerical simulations of gyroscopes were carried out using Simulink.

The rules for designing the fiber optic gyroscope basic construction are presented by Lefevre H.C. in [11]. A system analysis of the fiber-optic gyroscope is performed. The paper describes the basic principles underlying the fiber-

optic gyroscope, presents, and discusses methods for determining the characteristics of an object in space and the limits of the device operability.

Awrejcewicz J.'s study [12] is devoted to classical mechanics. Attention is focused on presenting a unique approach, introduced in classical mechanics, to the study of mechanical and electromagnetic processes occurring in applied mechanics and mechatronics. A special emphasis is placed on the theory, modeling, analysis and control of gyroscopic devices.

The parametric model construction of the tuning fork gyro using the universal Simulink tool was realized by Mohite S., Patil N., Pratap R. in [13]. The obtained results are compared with the data obtained using a more complex and powerful Coventor modeling system. The comparison shows that the parametric model created in Simulink gives equally good results with fractional effort in modeling and computation as the model built in Coventor. In most cases, finite element analysis is used in modeling.

Investigation of the vibration isolation platform design parameters at the time of gyro control is described by Yao Z., Jingrui Z., Shijie X in [14]. The vibration isolation is considered, as it provides a direct and effective approach to improving the high-precision guidance of high-resolution remote sensing. The paper presents studies that showed that the platform parameters satisfy the vibration isolation requirement, but also ensure that the control system remains fairly stable.

The main signs of the gyroscopes classification
Based on the existing gyroscopes structure and parameters analysis [9-13], a five-step classification of gyroscopes is proposed, which is shown in Figure 1.
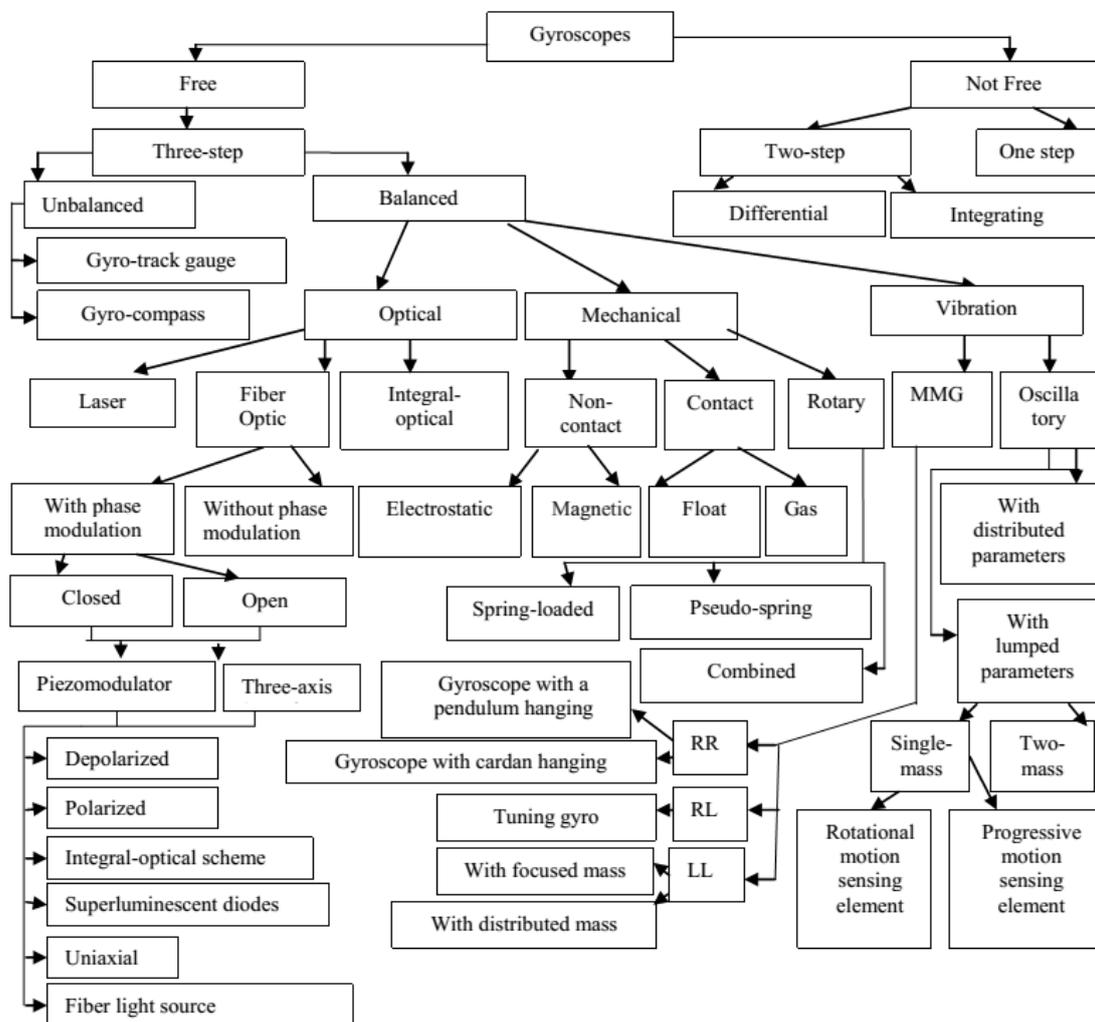
Fig–1: Classification of gyroscopes

In analyzing the features of modern gyroscopes, it is determined that all gyroscopes are subdivided into non-free (one- and two-stage gyroscopes) and free (three-stage gyroscopes) [13].

Free gyroscopes are divided into balanced, the center of rotors mass coincides with the rotors suspension center (a gyroscopes number built on the basis of balanced gyroscopes are called direction gyroscopes), and unbalanced, the mass center of which does not coincide with the suspension center are positional (heavy) gyroscopes.

All free gyroscopes, both balanced and unbalanced, have three identical properties: preserving property the orientation of its rotation axis invariance in space; processing property in the presence of an external force moment; property of insensitivity to impacts.

The basic types of gyroscopes in terms of the number of degrees of freedom can be divided into [10]: one step; two-step; three-step.

Gyroscopes with three degrees of freedom are divided into [2]: balanced or a static; unbalanced or positional.

Gyroscopes with two freedom degrees, in turn, are divided into [8]: differential gyroscopes; integrating gyroscopes.

Vibration gyroscopes combine devices that differ in the nature of the sensitive element (SE) motion and the principle of action, in which the moment (force) arises, causes the sensor to deviate from the institution that carries out the mobile movement. A distinguishing vibration gyroscopes feature is the connection of the sensitive element to the base on which it is mounted [8].

Optical gyroscopes have replaced old gyroscopes types, due to the fact that they have a number of advantages. In addition, these advantages have already created new gyroscopes areas application. Optical gyroscope has almost instant readiness to work, in comparison with mechanical. Such gyroscopes have much less weight, and high operation reliability due to the lack of mechanical elements.

There are fiber optic gyroscopes (FOG), which are manufactured in the so-called minimal configuration with equal optical paths for two rays propagating in the opposite direction, in the fiber circuit [8, 9].

Mechanical gyroscopes are based on the law of rotational moment (angular momentum) conservation. The main property of such a gyroscope is the ability to preserve in space the invariable direction of the rotation axis in the external forces acting absence on it and effectively resist the action of forces external moments. This property is largely determined by the magnitude of the gyroscope's own rotation angular velocity.

According to the principle of constructing an elastic suspension, all known MMG types can be classified depending on the SE motion type in the suspension, MMG can be divided into three groups [7-9]: MMG RR (rotare-rotare) type – both forms of oscillations are angular; MMG RL type – angular combination and linear form of rotor oscillations; MMG LL (linear-linear) type – both modes are linear.

Thus, a classification is presented, which consists of five levels, modern most common gyroscopes, allows determining their interrelationships. This makes it possible to study in more detail the gyroscopes structure, as well as their parameters.

RESULTS AND DISCUSSION
Parametric model of gyroscopes

Among the various microelectromechanical sensor systems, the gyroscope is one of the most complex sensors in terms of design, therefore on the basis of the presented classification it is proposed to develop a generalized parametric model. The parametric model includes the interrelationships of the it's various components parameters. In such a model, changing the value of one parameter entails changing the values of the gyroscope model parameters associated with it.

We construct a parametric description of each gyroscope separately set, which can be represented as:

$$G_k = < OG_i^j, MG_i^j, VG_i^j >, \tag{1}$$

where G_k – a lot of gyros at k – degrees number of freedom in a gyroscope, $k = 1...3$; OG_i^j – a subset of optical gyroscopes (Optical gyroscope), i = 1, 2, 3 this is the subclasses number; j – gyro parameters, $j = 1...n$; MG_i^j – a subset of mechanical gyroscopes (Mechanical gyroscope), i = 1, 2 this is the subclasses number, j – gyro parameters, $j = 1...n$; VG_i^j – a subset of vibration gyroscopes (Vibrating gyro), i = 1, 2, 3 this is the subclasses number, j – gyro parameters, where $j = 1...n$.

Let the subset of optical gyroscopes consist of structural elements:

$$OG_i^j = < R_{OG_i}, S_{OG_i}, LD_{OG_i}, U_{OG_i}, D_{OG_i}, OS_{OG_i} >, \tag{2}$$

where R_{OG_i} – reliability; S_{OG_i} – sensitivity; LD_{OG_i} – linear dimensions; U_{OG_i} – input voltage; D_{OG_i} – bandwidth; OS_{OG_i} – output signal.

Parameter R_{OG_i} reliability can be described as follows:

$$R_{OG_i} = < P(t)_{OG_i}, m_{OG_i}, Rf_{OG_i}, Pp(t)_{OG_i}, \lambda(t)_{OG_i}, Qp(t)_{OG_i} >, \tag{3}$$

where $P(t)_{OG_i}$ – trouble-free operation; m_{OG_i} – maintainability; Rf_{OG_i} – time to failure; $Pp(t)_{OG_i}$ – failure-free operation probability; $\lambda(t)_{OG_i}$ – failure rate, indicates the average failures number that occurs per unit of product operation time; $Qp(t)_{OG_i}$ – unexpected failure probability.

Parameter S_{OG_i} sensitivity can be represented as:

$$S_{OG_i} = < J_{OG_i}, \phi_{OG_i}, \kappa_{OG_i}, N_{OG_i}, a_{OG_i} >, \tag{4}$$

where J_{OG_i} – output signal; ϕ_{OG_i} – phase shift; κ_{OG_i} – proportionality coefficient, which is determined by the photodetectors parameter; N_{OG_i} – coil turns number; a_{OG_i} – an area that spans one turn.

Parameter J_{OG_i} (Output Signal) can be described as follows:

$$J_{OG_i} = < \phi_{OG_i}, \kappa_{OG_i}, I_{OG_i} >, \tag{5}$$

where ϕ_{OG_i} – phase shift; κ_{OG_i} – proportionality coefficient, which is determined by the photodetectors parameter; I_{OG_i} – light intensity at the radiation source output.

Parameter U_{OG_i} input voltage can be described as:

$$U_{OG_i} = < Ud_{OG_i}, Ks_{OG_i}, w_{OG_i}, N_{OG_i} >, \tag{6}$$

where Ud_{OG_i} – zero drift of the input signal; Ks_{OG_i} – scale gyro factor; w_{OG_i} – angular velocity; N_{OG_i} – noise gyro.

Let us now consider a mechanical gyroscopes subset consisting of structural elements:

$$MG_i^j = < R_{MG_i}, S_{MG_i}, E_{MG_i}, M_{MG_i}, \varphi_{MG_i}, L_{MG_i} >, \qquad (7)$$

where R_{MG_i} – reliability; S_{MG_i} – sensitivity; E_{MG_i} – exactness; M_{MG_i} – external force moment; φ_{MG_i} – deflection angle of the external suspension frame; L_{MG_i} – angular momentum.

Parameter R_{MG_i} reliability can be described as follows:

$$R_{MG_i} = < P(t)_{MG_i}, m_{MG_i}, Rf_{MG_i}, Pp(t)_{MG_i}, \lambda(t)_{MG_i}, Qp(t)_{MG_i} >, \qquad (8)$$

where $P(t)_{MG_i}$ – trouble-free operation; m_{MG_i} – maintainability; Rf_{MG_i} – time between failures; $Pp(t)_{MG_i}$ – probability of failure-free operation; $\lambda(t)_{MG_i}$ – the failure rate, indicates the average number of failures that occurs per unit of time; $Qp(t)_{MG_i}$ – probability of unexpected failure.

Parameter M_{MG_i} the moment of external force can be described as:

$$M_{MG_i} = < I_{i_{MG_i}}, \omega_{MG_i}, \varepsilon_{MG_i} >, \qquad (9)$$

where ε_{MG_i} – angular acceleration; $I_{i_{MG_i}}$ – moment of inertia relative to the rotation axis; ω_{MG_i} – angular velocity rotation vector.

Parameter L_{MG_i} the angular momentum consists of:

$$L_{MG_i} = < I_{i_{MG_i}}, \omega_{MG_i} > . \qquad (10)$$

The third gyroscope kind of is vibration gyroscopes. The subset consists of the following parametric elements:

$$VG_i^j = < E_{VG_i}, R_{VG_i}, S_{VG_i}, LD_{VG_i}, ME_{VG_i}, D_{VG_i}, V_{VG_i}, T_{VG_i} >, \qquad (11)$$

where E_{VG_i} – exactness; R_{VG_i} – reliability; S_{VG_i} – sensitivity; LD_{VG_i} – linear dimensions; ME_{VG_i} –measurement error; D_{VG_i} – durability; V_{VG_i} – maximum normal voltage; T_{VG_i} – torsions length.

Parameter R_{VG_i} reliability we express through:

$$R_{VG_i} = < P(t)_{VG_i}, m_{VG_i}, Rf_{VG_i}, Pp(t)_{VG_i}, \lambda(t)_{VG_i}, Qp(t)_{VG_i} >, \qquad (12)$$

where $P(t)_{VG_i}$ – trouble-free operation; m_{VG_i} – maintainability; Rf_{VG_i} – time to failure; $Pp(t)_{VG_i}$ – failure-free operation probability; $\lambda(t)_{VG_i}$ – failure rate; $Qp(t)_{VG_i}$ – unexpected failure probability.

Parameter D_{VG_i} durability we represent it in the form:

$$D_{VG_i} = <E_{VG_i}, N_{VG_i}, l_{VG_i}, \varepsilon_{VG_i}, p_{VG_i}>,\tag{13}$$

where E_{VG_i} – elastic modulus; N_{VG_i} – number of destruction cycles; l_{VG_i} – constants that are determined during the test; ε_{VG_i} – relative deformation; p_{VG_i} – oscillation frequency.

Parameter V_{VG_i} the maximum normal voltage is represented as:

$$V_{VG_i} = <M\max_{VG_i}, E_{VG_i}, J_{VG_i}, W_{VG_i}>,\tag{14}$$

where $M\max_{VG_i}$ – the maximum moment that occurs when the opposite end of the beam is displaced; E_{VG_i} – elasticity modulus of the beam material; J_{VG_i} – inertia moment of the cross-section beam; W_{VG_i} – resistance moment of in bending.

Parameter T_{VG_i} optimal length of elastic suspensions, torsions can be described as follows:

$$T_{VG_i} = <\lambda_{VG_i}, b_{VG_i}, c_{VG_i}, \varepsilon_{VG_i}, G_{tVG_i}, \omega_{VG_i}, p_{VG_i}>,\tag{15}$$

where λ_{VG_i} – torsion length; b_{VG_i} – thickness of torsions; c_{VG_i} – width of the torsions; ε_{VG_i} – elasticity modulus of silicon; G_{tVG_i} – torsion stiffness; ω_{VG_i} – resonance frequency in the driving mode; p_{VG_i} – operation frequency of the drive generator.

The proposed parametric model can be used as a basis for developing a mathematical model in the process of creating a module for the automated design of gyroscopes type: vibration, mechanical or optical.

Discussion of the results of the application of the parametric model for analyzing the performance of gyroscopes

With the proposed parametric model (8) for determining the micromechanical gyroscope parameters, studies were conducted of such parameters as the failure probability and the failure-free operation probability for different operating times. A gyroscope of the RR type is chosen for research.

The results of the calculations are given in Table 1 and Table 2.

The failure rate was determined on the basis of the expression [15]:

$$\lambda(t)_{MG_i} = \frac{f_{MG_i}(t)}{Pp(t)_{MG_i}} = \frac{c_1\lambda_1 e^{-\lambda_1 t} + c_2\lambda_2 e^{-\lambda_2 t}}{c_1 e^{-\lambda_1 t} + c_2 e^{-\lambda_2 t}} = \frac{n(t+\Delta t) - n(t)}{N(t)\cdot\Delta t}.\tag{16}$$

where $n(t)$ – number of failed products at time t; Δt – time interval; $N(t)$ – number of work items, by the time t.

The failure probability was calculated using the probability failure density, which is determined through the failure-free operation probability and the failure rate according to the formula [15]:

$$f_{MG_i}(t) = \frac{d\lambda(t)_{MG_i}}{dt}.$$ (17)

Table–1: Failure probability and failure-free operation probability for work over a period of 50 to 150 hours

Working hours t, h.	Failure probability $f_{MG_i}(t)$, %	Failure-free operation probability $Pp(t)_{MG_i}$, %
50	1.7	98.3
60	2.5	97.5
70	2.8	97.2
80	3.4	96.6
90	4.7	95.3
100	8.8	91.2
110	9.5	90.5
120	10.4	89.6
130	10.9	89.1
140	11.4	88.6
150	12.1	87.9

Now it is suggested to check the gyroscope operation after 20 hours.

Table–2: Failure probability and failure-free operation probability of for work over a period of 200 to 400 hours

Working hours t, h.	Failure probability $f_{MG_i}(t)$, %	Failure-free operation probability $Pp(t)_{MG_i}$, %
200	6.626	93.374
220	7.332	92.668
240	9.676	90.324
260	10.555	89.445
280	12.895	87.105
300	14.656	85.344
320	15.824	84.176
340	16.410	83.590
360	18.444	81.556
380	20.968	79.032
400	23.034	76.966

The failure-free operation probability is determined by the formula [15]:

$$Pp(t)_{MG_i} = e^{-\lambda t} = 1 - f_{MG_i}(t).$$ (18)

Dependence of the failure probability during the operation time from 50 to 150 hours is shown in Figure 2.
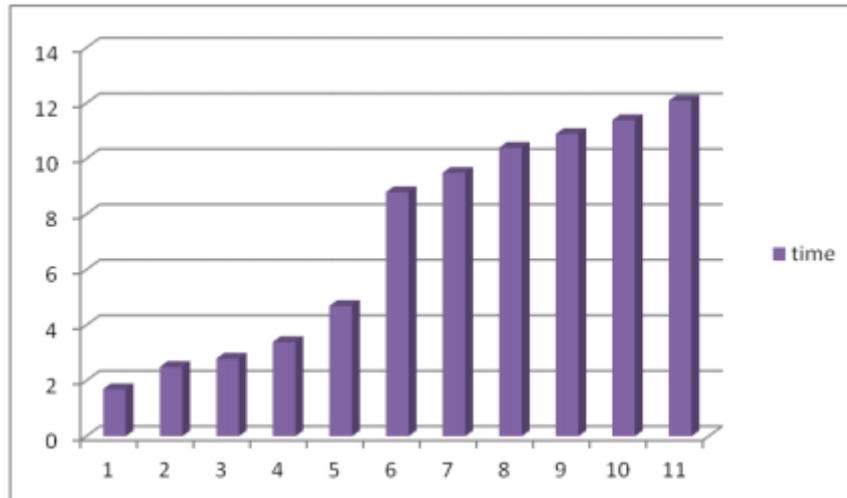
Fig–2: Dependence histogram of the failures probability on the operation time

In Figure 2 and Figure 3 on the abscissa axis 11 values – this is the operating time (from 50 to 150 hours with an interval of 10 hours).

Dependence of the failure-free operation probability during the operation time from 50 to 150 hours is shown in Figure 3.
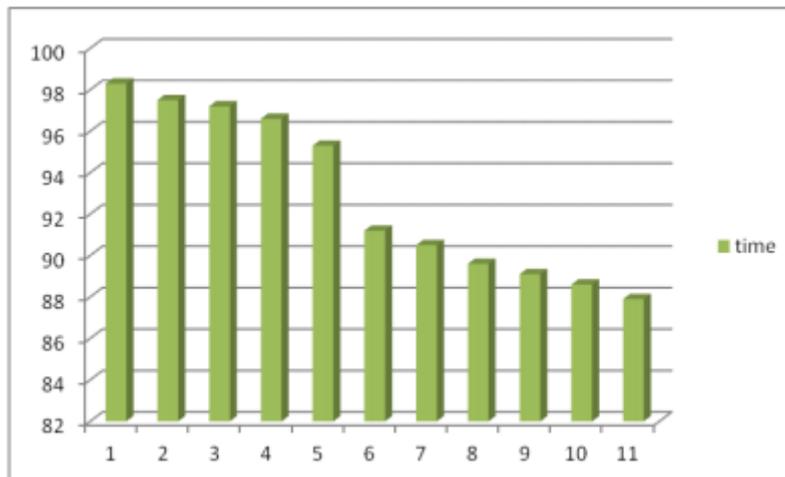
Fig–3: Dependence histogram of the of the failure-free operation probability on the operating time

The dependence of the failures probability and the failure-free operation probability on the operating time is shown in Figure 4 and Figure 5. In Figure 4 and Figure 5 on the abscissa axis 11 values – this is the operating time (from 200 to 400 hours with an interval of 20 hours).
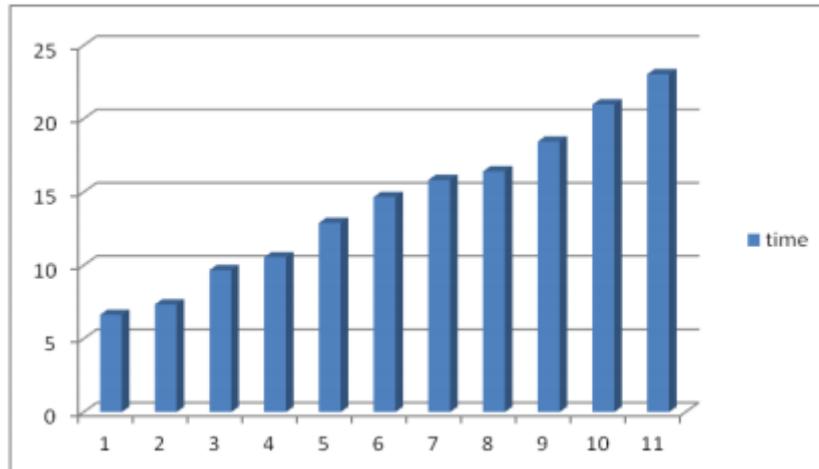
Fig–4: Dependence histogram of the failures probability on the operation time
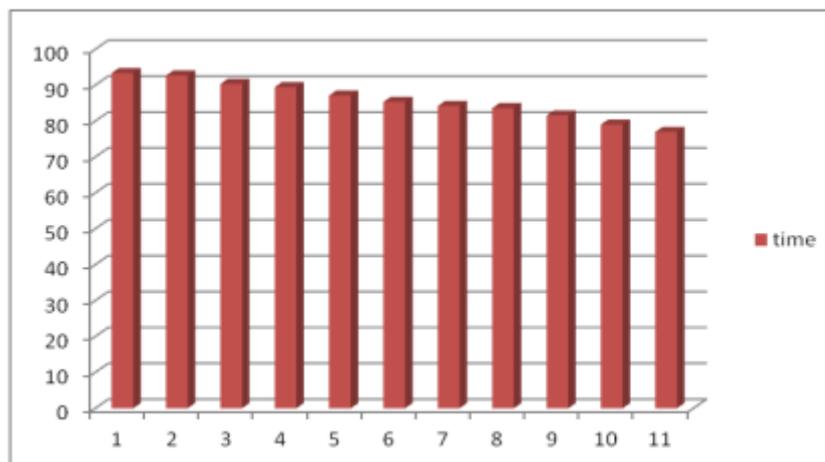
Fig–5: Dependence histogram of the of the failure-free operation probability on the operating time

The built-in histograms allow you to visualize the values of the selected micromechanical gyro parameters. On the basis of which it can be concluded that the longer the gyro operating time, the greater the failure probability and the lower the failure-free operation probability.

CONCLUSION

The structure of existing gyroscopes is reviewed; the gyro type's constructions and their functional capabilities are analyzed. The analysis made it possible to determine the main gyroscopes components and their parametric features, which subsequently became a prerequisite for the development of classification, as well as the creation of a parametric model.

A parametric model is proposed that can be used as a basis for developing a mathematical model in the process of creating a module for the automated gyroscopes design of vibration, mechanical or optical type.

As a result, the developed parametric model can be implemented in parametric methods in order to qualitatively pick up more structural gyroscopes elements, while considering different gyroscopes types, using always up-to-date data. Designed by the proposed models, the gyroscope will be more adapted to the environmental conditions and have optimal parameters for efficient operation of the device.

Investigations of the failure probability and the failure-free operation probability for a period of 50 hours to 150 hours and for a period of 200 hours to 400 hours were conducted. The longer the gyro worked the less chance of trouble-free operation.

ACKNOWLEDGMENT

REFERENCES

1. Kuznetsov AG, Molchanov AV, Chirkin MV, Izmailov AE. Precise laser gyroscope for autonomous inertial navigation. Quantum Electronics. 2015;45: 78-79.
2. Hu ZX, Gallacher BJ, Burdess JS, Bowles SR, Grigg HTD. A systematic approach for precision electrostatic mode tuning of a MEMS gyroscope. Journal of Micromechanics and Micro engineering. 2014;24(12):125003.
3. Eling C, Klingbeil L, Wieland M, Kuhlmann H. A precise position and attitude determination system for lightweight unmanned aerial vehicles. Int. Arch. Photogramm. Remote Sens. Spatial Inf. Sci. 2013.
4. Bereska D, Daniec K, Fraś S, Jędrasiak K, Malinowski M, Nawrat A. System for multi-axial mechanical stabilization of digital camera. In Vision Based Systemsfor UAV Applications. 2013: 177-189.
5. Reze M, Osajda M, Halbleiter F. MEM's sensors for automotive vehicle stability control applications. Mems for Automotive and Aerospace Applications. 2013:29.
6. Antonello R, Oboe R. Exploring the potential of mems gyroscopes: Successfully using sensors in typical industrial motion control applications. IEEE Industrial Electronics Magazine. 2012;6(1):14-24.
7. Kumar S, Hemalatha B. Design and Simulation of MEMS Based Gyroscope. IOSR Journal of Electrical and Electronics Engineering. 2013;5(6):22-30/
8. Pai P, Chowdhury FK, Mastrangelo CH, Tabib-Azar M. MEMS-based hemispherical resonator gyroscopes. In Sensors, 2012:1-4).
9. Dellea S, Giacci F, Longoni AF, Langfelder G. In-plane and out-of-plane MEMS gyroscopes based on piezoresistive NEMS detection. Journal of microelectromechanical systems, 2015; 24(6):1817-1826.
10. Yilmaz E. Design, analysis and simulation of microscale solid-wave gyroscopes. 2016.
11. Lefevre HC The fiber-optic gyroscope. Artech house. 2014.
12. Awrejcewicz J. Classical mechanics: kinematics and statics. Springer Science & Business Media. 2012.
13. Mohite S, Patil N, Pratap R. Design, modelling and simulation of vibratory micromachined gyroscopes. Journal of Physics: Conference Series. 2006; 34(1): 757.
14. Yao Z, Jingrui Z, Shijie X. Parameter's design of vibration isolation platform for control moment gyroscopes. Acta Astronautica. 2012;81(2):645-659.
15. Gnedenko BV, Belyayev YK, Solovyev AD. Mathematical methods of reliability theory. Academic Press. 2014.
16. Lyashenko V, Ahmad MA, Sotnik S, Deineko Zh, Khan A. Defects of Communication Pipes from Plastic in Modern Civil Engineering. International Journal of Mechanical and Production Engineering Research and Development. 2018;8(1):253-262.
17. Lyashenko V, Ahmad MA, Kobylin O, Khan A. Study of Composite Materials for the Engineering using Wavelet Analysis and Image Processing Technology. International Journal of Mechanical and Production Engineering Research and Development. 2017;7(6):445-452.
18. Sotnik S, Matarneh R, Lyashenko V. System Model Tooling For Injection Molding. International Journal of Mechanical Engineering and Technology. 2017;8(9):378–390.
19. Khan A, Joshi S, Ahmad MA, Lyashenko V. SomeEffect of ChemicalTreatment by Ferric Nitrate Salts on the Structure and Morphology of Coir Fibre Composites. Advances in Materials Physics and Chemistry. 2015;5(01):39-45.
20. Ahmad MA, Lyashenko VV, Lyubchenko VA, Khan A, Kobylin OA. The Methodology of Image Processing in the Study of the Properties of Fiber as a Reinforcing Agent in Polymer Compositions. International Journal of Advanced Research in Computer Science. 2016;7(1):15-18.
21. Lyashenko VV, Ahmad MA, Lyubchenko VA, Khan A, Kobylin OA. Image Processing a New Era in the Study of Natural Polymer Composites. Asian Academic Research Journal of Multidisciplinary. 2016;3(3):288-300.
22. Putyatin YP, Ahmad MA, Lyashenko VV, Khan A. The Pre-Processing of Images Technique for the Material Samples in the Study of Natural Polymer Composites. American Journal of Engineering Research. 2016;5(8): 221-226.
23. Lyashenko V, Kobylin O, Ahmad MA. General Methodology for Implementation of Image Normalization Procedure Using its Wavelet Transform. International Journal of Science and Research (IJSR). 2014;3(11):2870-2877.